Exploring future large-scale ROADM architectures

Diogo C. Morão[2], Luís G. Cancela[1,2], and João L. Rebola[1,2]
[1]Optical Communications and Photonics Group, Instituto de Telecomunicações, Lisboa, Portugal
[2]Department of Science and Information Technology, Instituto Universitário de Lisboa (ISCTE-IUL), Lisboa, Portugal
Emails: dmcmo@iscte-iul.pt; luis.cancela@iscte-iul.pt; joao.rebola@iscte-iul.pt

***Abstract*—Most of today's optical networks are based on reconfigurable optical add/drop multiplexers (ROADMs) nodes. However, current ROADM architectures have poor scalability due to limitations on the wavelength selective switches dimension. Hence, due to the constant increase in data traffic and the demand for more dynamic and flexible networks, current architectures might become a bottleneck in the foreseen large-scale ROADMs. In this work, several architectures for large-scale ROADMs proposed to overcome this bottleneck are studied in terms of hardware cost and in-band crosstalk generation and compared with large-scale ROADMs built with conventional architectures. We show that ROADMs based on a sub-system modular architecture, also known as interconnected architecture, exhibit a significant hardware cost reduction in relation to conventional architectures and are also advantageous regarding the in-band crosstalk generation. Moreover, in this work, an analysis of optical filtering effects, amplified spontaneous emission noise and in-band crosstalk impact in the performance of an optical network, with nodes based on the interconnected architecture, is performed through Monte-Carlo simulation.**

***Keywords*—amplified spontaneous emission noise, bank based add/drop, in-band crosstalk, large-scale ROADMs, optical filtering.**

I. Introduction

Optical networks are continually evolving in order to accommodate all the huge amount of traffic that flows through it. Nowadays, a highly flexible and dynamic network, with an increasing transport capacity, is required to accommodate such amount of traffic [1].

Hence, all optical network components and ROADM nodes must be improved to meet such characteristics. The future deployment of large-scale ROADMs, implemented with currently available components can become very complex since large dimension wavelength selective switches (WSS) have to be built by cascading smaller WSSs. New ROADM architectures have been proposed in order to reduce the dimension of the components and therefore make the large-scale ROADMs more feasible to manufacture and deploy [2], [3].

Moreover, in these large-scale ROADMs, optical physical layer impairments (PLIs) require a more in-depth analysis, because the optical signal, along its light path, passes through optical fiber links as well as many network components within ROADMs, such as optical switches, WSS and splitters/couplers. As a result, the impact of insertion losses, optical filtering effects, amplified spontaneous emission (ASE) noise and in-band crosstalk in large-scale ROADM components, on the performance of the optical signal along its lightpath inside the optical network is still to be investigated.

In this work, we study the large-scale ROADMs architectures proposed in [3] and [4], respectively, named as interconnected A or B and FLEX architectures, in terms of hardware cost and in-band crosstalk generation and compare these findings with the ones obtained for conventional large-scale ROADM architectures. The add/drop (A/D) structure proposed in [4] is also explored and compared with traditional A/D structures. Then, we assess the impact of the PLIs, in particular of cascading optical filters, ASE noise accumulation and in-band crosstalk generated inside the interconnected A based ROADMs with bank-based A/D structures on the network performance through Monte-Carlo simulation. We consider polarization division multiplexing 16- and 32- quadrature amplitude modulation (PDM-QAM) signals, respectively, with 200 Gb/s and 250 Gb/s. This study is performed by properly modelling large-scale ROADM nodes, considering both broadcast and select (B&S) and route and select (R&S) architectures.

This work is organized as follows. In Section II several large-scale ROADM architectures are described and compared in terms of the hardware cost with conventional B&S and R&S ROADM architectures. In Section III a comparison in terms of number of in-band interferers is performed for the studied architectures. Section IV presents the network performance assessment taking into account the influence of the studied PLIs. Section V presents the main conclusions of this work.

II. Large scale ROADM architectures

In this section, large-scale ROADM architectures based on a sub-system modular architecture and also architectures based on grouping wavelengths together to be switched as a whole signal are presented and compared in terms of hardware cost with conventional large-scale ROADMs architectures.

A. Conventional ROADM architectures

The conventional ROADM architectures considered in this work are the B&S and R&S [5]. In a conventional B&S architecture, the optical input signal is sent to all ROADM degrees (outputs) via an optical splitter. Each output WSS then selects which wavelength to transmit. In a conventional R&S architecture, instead of broadcasting the optical input signal, there is a selection of the signal using a "route" WSS. Thus, there are two phases of wavelength selection, at the ROADM input and at the output. For this reason, the signal goes through one more filtering stage than in the conventional B&S architecture.

For a ROADM node size (K) whose degrees (D) have multiple fibers (f_D), where $K = f_D \times D$, or a single fiber ($f_D = 1$) with a higher degree number (e.g. $D \geq 16$), the resulting architectures can become quite complex because large port-count WSSs are difficult to manufacture since the highest port count WSS commercially available is a 1×35 [6]. Nevertheless, a large port-count WSS can be built by cascading multiple WSSs using an optical splitter, or a smaller WSS, that splits the signal to the n cascaded WSSs [3]. This solution, however, significantly increases the ROADM hardware cost. The number of WSSs, n, required to build a cascaded WSS is $\lceil K/D_L \rceil$ [2] , where D_L is the size of each WSS. The total number of WSSs required to build cascaded WSSs for the two conventional architectures, W_{conv}, is therefore $C_f \times K \times n$, where C_f is 1 or 2, respectively, for B&S or R&S architectures.

B. Interconnected ROADM sub-systems architecture

A ROADM architecture named interconnected ROADM sub-systems has been proposed to reduce the WSSs number and size required to implement large-scale ROADMs [2], [4], [7]. This proposed architecture has two possible solutions, interconnected A, shown in Fig. 1 and interconnected B. Interconnected A architecture (Fig. 1) consists of multiple interconnected small ROADM sub-systems, whose port count is much lower than the cascaded port count WSS (D_L) used in conventional large-scale ROADMs. Each ROADM sub-system is a conventional ROADM architecture, B&S or R&S, but with smaller size ($D_S \times D_S$). Recently, there is also the possibility to use $M \times M$ WSSs as ROADM sub-systems [7]. The node has K pairs of inter-node fibers that connect that node to the others and each ROADM sub-system has $2f_{intra}$ pairs of intra-node fibers that inter-connect adjacent ROADM sub-systems, where f_{intra} denotes the number of fibers connected to an adjacent ROADM sub-system. When entering or exiting the network, the signal is sent from/to the A/D structure using a 1×2 WSS, before entering/exiting the ROADM through one sub-systems port. The signal can be routed through a maximum number of ROADM sub-systems, known as hop slug, n_{hops}, whose typical value is 2 [2].

The total number of ROADM sub-systems in an interconnected A architecture node, N_{SUB_A}, is given by $\lceil K/(D_S - 2f_{intra}) \rceil$.

To build a $K \times K$ ROADM, the number of WSSs needed to interconnect the sub-systems together, N_{inter}, is given by $2f_{intra} \cdot N_{SUB}$ and, therefore, the total number of WSSs required to build an interconnected A architecture, W_{inter_A} is given by $C_f \times (K + N_{inter})$.

The major advantage of this structure is the possibility of building large-scale ROADMs using small port-count WSSs (D_s), that are more accessible and feasible than larger ones, which are required in large-scale conventional ROADMs [2].

The difference in interconnected A and interconnected B architectures is that the A/D structure, in the latter, is connected directly to the ROADM sub-systems, hence sharing the routing ability, i.e., a signal added in a given ROADM sub-system can exit the ROADM in a different ROADM sub-system [4]. Half the sub-systems inputs are reserved to the A/D signals and the other half to express signals, hence, this architecture requires twice the number of WSSs, W_{inter_B}, given by $C_f \times (2K + N_{inter})$.

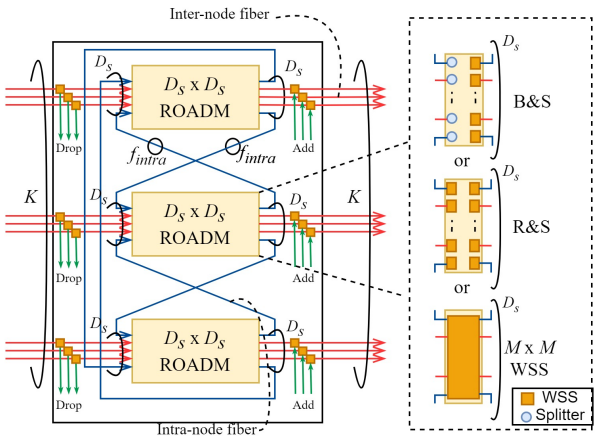

FIG. 1: Interconnected A ROADM sub-systems node architecture [2], [7].

C. FLEX architecture

Recently, another architecture, known as FLEX, has been proposed as a solution to deploy large-scale ROADMs with high port count WSSs [3]. In the FLEX architecture, the wavelength division multiplexing (WDM) signals from the several input directions are grouped together in W_B groups and then switched to one of the output fibers, as a whole signal. This architecture is composed of small-port-count $2 \times K$ WSSs with dimension $1 \times W_B$ and W_B $K \times K$ matrix switches.

D. Hardware cost comparison

In this subsection, the conventional, interconnected and FLEX architectures are compared, in terms of the number of WSSs required to achieve a 80×80 ROADM using different WSS sizes. Today, WSS with sizes of 1×2, 1×4, 1×9, 1×20 or 1×35 are typically available [6].

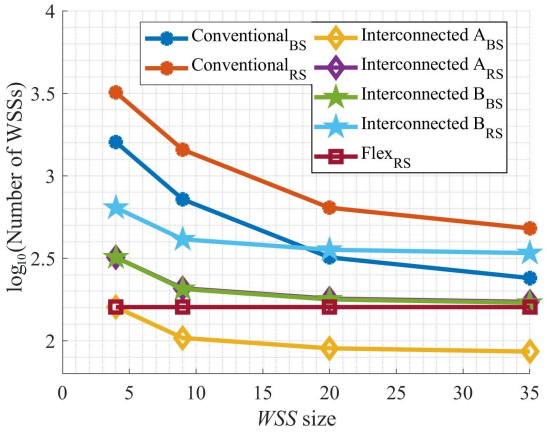

FIG. 2: Number of required WSSs, as a function of the WSS size, for 80×80 ROADMs, considering different express architectures.

In Fig. 2, the number of WSSs required as a function of the WSS size is represented for a ROADM size of $K = 80$ for each architecture, considering both B&S and R&S architectures, except for the FLEX architecture which has only the R&S architecture option [3]. Also, for the interconnected architecture, both A and B implementations are considered. For all the ROADM sizes, the number of WSSs is represented in logarithmic scale. We have considered $W_B = 4$ for the FLEX architecture [3].

For a large-scale ROADM of 80×80, the three studied architectures look more promising in reducing the number of WSS required, as shown in Fig. 2. Note that the interconnected A_{RS} line is superimposed with the interconnected B_{BS} line. For WSS sizes below 1×20, the interconnected A, B and FLEX architectures require 10 times less WSSs than conventional nodes (B&S or R&S). For WSS sizes of 1×20 and 1×35, the WSS number is reduced only 2 times. Thus, we can conclude that the three studied architectures are a feasible solution to build large-scale ROADMs, since they reduce the number of WSSs.

E. Bank-based A/D architecture

To reduce the hardware cost of the A/D structure, a bank based A/D structure has been proposed in [4], whose architecture is shown in Fig. 3.

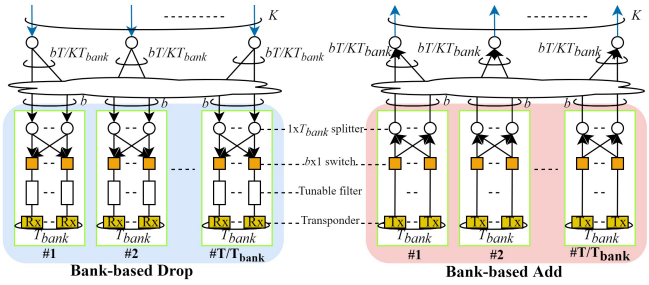

FIG. 3: Bank-based A/D architecture.

When dropping a signal, a "feeder" splitter distributes the dropped signals to bT/KT_{bank} banks out of T/T_{bank} total banks, where T is the total number of transponders, T_{bank} is the number of transponders in one bank and b is the number of input/output fibers of each bank [4]. Although there are no restrictions within each bank, only a limited number of A/D fibers can be accessed by each bank [4].

In the bank-based A/D stage, routing flexibility and hardware requirements can be controlled by the parameter b. Smaller b enables fewer optical amplifiers (OAs) due to reduced splitter losses, while larger b offers reduced signal A/D blocking, as the number of banks that can connect to each A/D fiber increases [4].

In order to compare the bank-based structure to the conventional A/D structure, we have analysed different values of T_{Bank} and b and concluded that $T_{Bank} = 32$ and $b = 8$ is the configuration that reduces most the hardware cost. If we consider a 80×80 ROADM, with 20% A/D ratio, a total of 1536 transponders is required, for each A/D stage, and 1536 tunable filters for the drop stage. For a conventional colorless, directionless and contentionless (CDC) drop stage, 4000 1×32 splitters and 3920 OAs are required, as well as 1536 80×1 switches. With the bank-based A/D stage, considering T_{bank}=32, T=1536 and b=8, only 80 1×8 "feeder" splitters and 384 1×32 "bank" splitters are required. The switch size and OAs needed are significantly smaller, 1×8 and 464, respectively. This represents a large reduction of 88% in the number of OAs and 88% in optical splitters.

III. IN-BAND CROSSTALK GENERATION IN LARGE-SCALE ROADMS

In this section, the number of in-band crosstalk signals is analysed for all studied architectures considering a worst-case scenario. The expressions for obtaining the number of crosstalk signals are given in Table I. For interconnected ROADM architectures, we have considered $n_{hops} = 2$ and $f_{intra} = 1$, which are typical values.

TABLE I: Number of in-band crosstalk signals originated in the express ROADM architecture.

	Broadcast&Select	
	1^{st} order	2^{nd} order
Conventional Node	$K-1$	-
Inter-Connected A*	$3D_S-7$	$4D_S-10$
Inter-Connected B*	$3D_S-7$	$4D_S-10$
FLEX - Waveband	N/A	N/A

	Route&Select	
	1^{st} order	2^{nd} order
Conventional Node	-	$K-1$
Inter-Connected A*	-	$3D_S-7$
Inter-Connected B*	-	$3D_S-7$
FLEX - Waveband	$K-1$	$(K-1)\times(W_B-1)$

* This only applies to $N_{SUB} \geq 7$.

As observed in Table I, FLEX architecture with a R&S configuration and a typical $W_B = 4$ [3], has the worst performance in terms of the number of in-band crosstalk terms, having a similar number of first order interferers than the conventional B&S architecture. The in-band crosstalk generation in the interconnected ROADM architectures is independent of the ROADM size. For these architectures, D_S sizes of 6 and 9 are commonly used [2], [8].

We conclude that for large-scale ROADMs, such as $K = 80$, the interconnected A or B with R&S architecture are the best choice in terms of in-band crosstalk, because all interfering terms, 20 for $D_s = 9$, are second order interferers. Furthermore, the number of interferers depends only on D_s and not on the ROADM dimension, K. For the same scenario, the conventional R&S architecture has 79 second-order interferers.

TABLE II: Number of in-band crosstalk terms originated in the ROADM A/D structure.

	Drop ports		Add ports	
	1^{st} order	2^{nd} order	1^{st} order	2^{nd} order
A/D with MCS	K-1	-	K-1	-
A/D with WSS	-	K-1	-	K-1
Bank Based	$b-1$	-	$\frac{bT}{KT_{bank}} \times (b-1)$	-

Table II summarizes the expressions used to calculate the number of in-band crosstalk terms in both conventional CDC A/D and bank-based A/D structures.

As a numerical example, a 20% A/D ratio 80×80 ROADM with a conventional A/D structure using multicast switches (MCSs), generates 79 1^{st} order in-band crosstalk terms in both drop and add ports, while in bank-based A/D architecture considering $b = 8$ and $T_{bank} = 32$, the number of in-band crosstalk terms drops to 7, in the drop ports, and 35, in the add ports. This is a significant performance improvement for large-scale ROADMs in terms of the in-band crosstalk impairment, representing a 90% and a 55% decrease, for the drop and add ports, respectively, in a bank-based architecture in comparison to conventional MCS architecture. Also, in comparison with a conventional WSS A/D architecture, the number of in-band crosstalk terms in the bank-based has also a 90% and a 55% decrease, for the drop and add ports, respectively. However, the in-band crosstalk terms are 2nd order terms in the conventional WSS architecture.

IV. Network Performance Assessment in the Presence of Physical Layer Impairments

The goal of this section is to assess the network performance using interconnected A architecture ROADMs with bank/based A/D through Monte-Carlo simulation. First, optical filtering effects and ASE noise accumulation are studied, and then, the in-band crosstalk is added to the simulator. The results presented are valid for $K \geq 49$ and $D_s = 9$.

A. Impact of optical filtering and ASE noise in a cascade of ROADM nodes with lumped amplification

In this subsection, the impact of ASE noise arising from lumped amplification on a network composed by cascaded interconnected A ROADMs architecture nodes, using the bank-based A/D structure, is analysed. We considered that the reference scenario corresponds to a signal that travels only through 2 nodes, the add node and the drop node. This scenario is depicted in Fig. 4, considering that the 1^{st} *K*-scale ROADM is connected directly to the last *K*-scale ROADM (i.e., neglecting the express ROADMs). The corresponding amplification stages and amplifier characteristics are also depicted. The signal enters the network in the add structure followed by an OA, with small gain of 3 dB or 5.7 dB, respectively, for B&S and R&S architectures, that partially compensates the add losses, and a 2×1 WSS that makes the connection between the add stage and the express path. After this WSS, a post-amplifier, G_{post}, with a 30.6 dB or 28 dB gain, respectively, for B&S and R&S architectures, compensates the express path losses and uncompensated add losses. At the input of the last node, there is a pre-amplifier, G_{pre}, with a 12.5 dB gain that fully compensates the fiber losses. Since the signal is to be dropped, it is sent to the drop structure by a 2×1 WSS. In our case, the drop losses are very high (33.7 dB) and an OA to compensate them would generate too much noise, hence, we use 2 OAs in a multi-stage configuration at the drop node. In this way, the signal then passes by an OA named G_{drop1}, with a 16.6 dB gain, and then goes to the bank-based drop structure, where before entering the bank, the losses are compensated by a second OA named G_{drop2}, with a 17 dB gain.

When the number of ROADM nodes is larger than two, the model considered for the express nodes in Fig. 4 is depicted inside the dashed blue line box, wherein each express node between the first and last nodes, the signal goes through a pre-amplifier and a post-amplifier, and also 2 more OAs named G_{inter}, with 16.6 dB or 14 dB gain, respectively, for B&S and R&S architectures, that compensate the losses between the ROADM sub-systems. In all subsequent studies, we always consider that $n_{hops} = 2$ (i.e., the worst case).

The additional simulation parameters considered are presented in Table III.

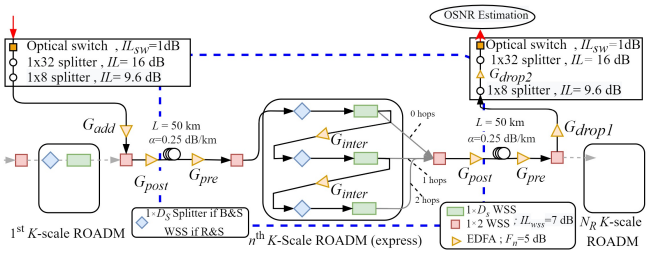

FIG. 4: Simulation model of the optical network to study the accumulation of ASE noise and optical filtering impact.

TABLE III: Additional MC simulation parameters.

Signal modulation format	16QAM, 32QAM	
Symbol rate	R_s	32 Gbaud
Target bit error rate	BER	10^{-2}
WDM channel spacing	Δf	50 GHz
Number of channels	N_{ch}	96
Number of transponders per bank	T_{bank}	32
Number of input fibers per bank	b	8
Number of hops between sub-systems	n_{hops}	2
Sub-system dimension	D_s	9

To study the network performance we consider two design considerations. First, we set the maximum signal power per WDM channel, $P_{max_{ch}}$, by considering a power level of 1 dBm at each ROADM input [9]. The second design rule is to consider a safety margin, SM, to the optical signal-to-noise ratio (OSNR) at the receiver in order to account for additional system performance degradation caused by, for example, crosstalk between carriers and material aging [9]. The SM is defined in [9], and we consider the intercarrier crosstalk penalty as 0.5 dB, and set the optical filtering penalty to 0 dB, since it is already included in our simulator. A residual margin of 0 dB is also considered. The MC simulation is performed as in [10] and the ASE noise and optical filter models are found in [11] and [12], respectively.

In order to address the maximum reach in terms of cascaded ROADM nodes, the OSNR at the optical receiver input and the required signal power at the transmitter for a bit error rate (BER) of 10^{-2} as a function of the number of ROADM nodes traversed is shown in Figs. 5 a) and b), respectively. In Fig. 5 a), the solid lines represent $OSNR_{tot}$, the total required OSNR including the safety margin, and the dashed lines show the required OSNR, $OSNR_{req}$, including the optical filtering and the ASE noise accumulation. In order to obtain the OSNRs

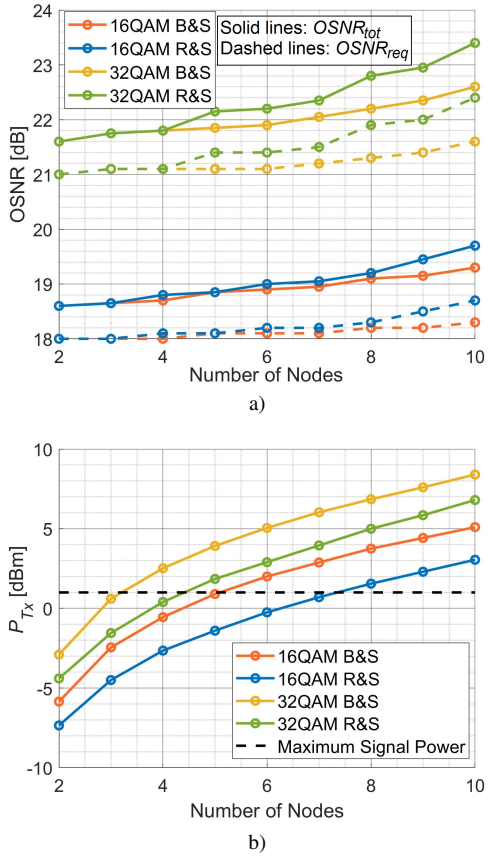

FIG. 5: Required OSNR at the optical receiver input a) and transmitted signal power b) as a function of the number of cascaded interconnected A nodes.

accounting the additional margin, $OSNR_{tot}$, the transmitted signal powers must be raised to the levels depicted in Fig. 5 b), for each number of nodes considered. The constraint regarding the maximum signal power of 1 dBm at the ROADM inputs is also plotted using a dashed black line. Since the optical link losses are fully compensated, the signal power at the optical transmitter output, P_{Tx}, is equal to the signal power at the ROADM inputs. The optical filtering penalty can be extracted from Fig. 5 a), by subtracting the OSNR obtained for a specific number of cascaded nodes by the OSNR obtained for the reference situation of 2 nodes. The optical filtering penalty for 10 nodes is 0.4 dB and 0.8 dB, respectively, for a 16QAM and 32QAM signal in a B&S architecture, and 0.7 dB and 1.4 dB, respectively, for a 16QAM and 32QAM signal in a R&S architecture.

From Fig. 5 b), and considering 1 dBm signal power per channel as the limiting power, it can be concluded that the 16QAM signal allows a higher network reach of 5 and 7 nodes, while the 32QAM only allows 3 and 4 cascaded nodes, respectively, for B&S and R&S architectures. The higher modulation format, 32QAM, as expected [13], is less resilient to node cascading, mainly due to the higher signal power required to achieve the target BER, in the reference scenario, which reduces the OSNR budget. The B&S architecture leads to a lower reach in comparison with the R&S architecture due to the ASE noise power generated along the optical path, whose effect in the performance degradation is stronger than the optical filtering penalty.

B. Impact of in-band crosstalk in a cascade of ROADM nodes with lumped amplification

In this subsection, the in-band crosstalk impairment is added to the simulation model and its impact on a network composed by a cascade of interconnected A ROADM sub-systems architecture nodes using the bank-based A/D structure is analysed.

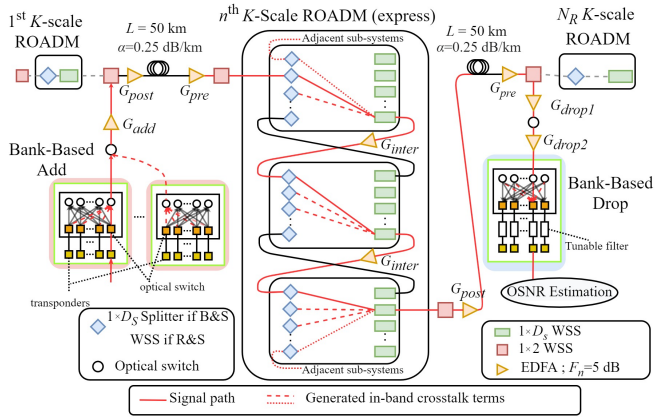

FIG. 6: Simulation model of the optical network to study the in-band crosstalk impact.

The interfering in-band signals follow the same path of the primary signal in the optical network as depicted in Fig. 6. The number of in-band crosstalk signals originated in the A/D structure depends on the bank-based structure parameters, while the ones originated in express ROADMs differ in case of B&S or R&S configurations. As presented in Table I, we expect that the in-band crosstalk penalty is higher in the B&S interconnected A, which has first order interferers, while the R&S interconnected A architecture has only second order interferers. The isolation level considered for the optical switches existing in the MCS and the blocking amplitude for the WSSs is -60 dB and -40 dB, respectively [14], [15].

Fig. 7 a) shows the total OSNR (including the safety margin) as a function of the number of nodes, for 16 and 32QAM and the B&S and R&S architectures. The OSNR with and without crosstalk is depicted. Fig. 7 b) shows the signal power at the transmitter output required to reach the corresponding total OSNR with in-band crosstalk.

As depicted in Fig. 7, the system performance is also evaluated by assessing the network maximum reach considering a maximum signal power per channel of 1 dBm and by setting a safety margin on the required OSNR. The in-band crosstalk OSNR penalty can be extracted from Fig. 7 a) from the difference between the solid and dashed lines for each modulation and architecture configuration. The R&S architecture shows a negligible in-band crosstalk penalty. For 10 cascaded nodes, the OSNR penalty is 1.7 dB and 3 dB, respectively, for 16QAM and 32QAM signals, considering a B&S architecture.

In Fig. 7 b), it is shown that regardless of the modulation format, the B&S architecture leads to a lower reach in compar-

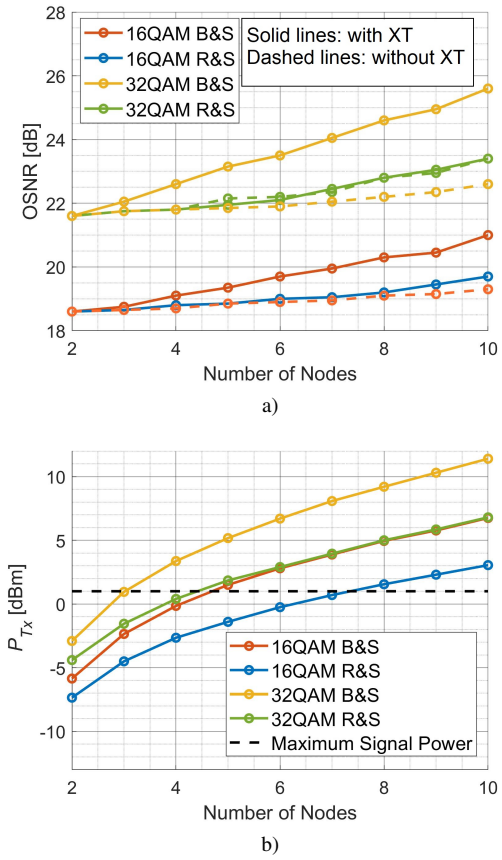

FIG. 7: OSNR, with and without in-band crosstalk, at the optical receiver input including the safety margin a) and transmitted signal power b) as a function of the number of cascaded interconnected A nodes with 2 hops in both B&S and R&S configurations with the presence of in-band crosstalk.

ison with the R&S and, that, the 16QAM signal allows a higher network reach of 4 and 7 cascaded nodes, while the 32QAM allows only 3 and 4 cascaded nodes, respectively, for B&S and R&S architectures. The maximum reach of a network with in-band crosstalk in comparison with network reach without in-band crosstalk is similar, and the only difference is in the 16QAM signal with B&S interconnected A nodes that reduce from 5 (Fig. 5 b)) to 4 (Fig. 7 b)) cascaded nodes. This maximum reach after a few cascaded nodes results from a compromise between the maximum signal power per channel at the ROADM inputs and the stronger influence of the ASE noise in comparison with the effect of in-band crosstalk and optical filtering.

V. CONCLUSIONS

In this work, several architectures for future large-scale ROADMs have been studied and its performance has been assessed, considering the impact of optical filtering, ASE noise and in-band crosstalk. It is shown that the interconnected A architecture with the bank-based A/D structure represents a feasible solution to reduce the hardware cost and in-band crosstalk generation in comparison with large-scale ROADMs based on conventional architectures, and also in comparison with the interconnected B and Flex architectures.

In particular, for a large-scale ROADM with an 80x80 dimension, using WSS sizes below 1x20, it is shown that the interconnected A architecture requires 10 times less WSSs than conventional nodes (B&S or R&S). Moreover, it is also shown that the A/D bank-based structure can achieve a large reduction of 88% in the number of OAs and 88% in optical splitters in comparison with conventional A/D structures. Regarding the influence of the PLIs in the large-scale ROADMs investigated in this work, our Monte-Carlo simulation results have shown that the maximum reach of a 16QAM signal is 4 and 7 nodes, respectively, for B&S and R&S architectures. A 32QAM signal, has a lower reach of 3 and 4 nodes, respectively, for B&S and R&S architectures.

ACKNOWLEDGMENT

This work was supported under the project of Instituto de Telecomunicações UIDB/EEA/50008/2020.

REFERENCES

[1] S. Gringeri, B. Basch, V. Shukla, R. Egorov, and T. Xia, "Flexible Architectures for Optical Transport Nodes and Networks," *IEEE Commun. Mag.*, vol. 48, no. 7, pp. 40–50, July 2010.

[2] Y. Iwai, H. Hasegawa, and K.-I. Sato, "OXC Hardware Scale Reduction Attained by Using Interconnected Subsystem Architecture," *Optical Fiber Communication Conference and Exhibition (OFC)*, Anaheim, CA, USA, March 2013, paper NW1J.2.

[3] H. Hasegawa, S. Subramaniam, and K.-I. Sato, "Node Architecture and Design of Flexible Waveband Routing Optical Networks," *IEEE J. Opt. Commun. Netw*, vol. 8, no. 10, pp. 734–744, October 2016.

[4] M. Niwa, Y. Mori, H. Hasegawa, and K.-I. Sato, "Tipping Point for the Future Scalable OXC: What Size M×M WSS Is Needed?," *IEEE J. Opt. Commun. Netw*, vol. 9, no. 1, pp. A18–A25, January 2017.

[5] J. M. Simmons, *Optical Network Design and Planning*. Springer, 2nd ed., 2014.

[6] Lumentum, "Optical Communications Products." Available: https://www.lumentum.com/en/optical-communications/all-products, 2019.

[7] M.-E. Ganbold, T. Yasuda, Y. Mori, H. Hasegawa, and K.-I. Sato, "Assessment of Optical Cross-Connect Architectures for the Creation of Next Generation Optical Networks," *2018 23rd Opto-Electronics and Communications Conference (OECC)*, Jeju, Korea, July 1 2018.

[8] R. Hashimoto, S. Yamaoka, Y. Mori, H. Hasegawa, K.-I. Sato, K. Yamaguchi, K. Seno, and K. Suzuki, "First Demonstration of Subsystem-Modular Optical Cross-Connect Using Single-Module 6 × 6 Wavelength-Selective Switch," *J. Lightwave Technol.*, vol. 36, no. 7, pp. 1435–1442, April 1 2018.

[9] J. Pedro, "Designing Transparent Flexible-Grid Optical Networks for Maximum Spectral Efficiency," *IEEE J. Opt. Commun. Netw.*, vol. 9, no. 4, pp. C35–C44, April 2017.

[10] B. R. Pinheiro, J. L. Rebola, and L. G. C. Cancela, "Impact of In-Band Crosstalk Signals with Different Duty-Cycles in M-QAM Optical Coherent Receivers," *2015 20th European Conference on Networks and Optical Communications - (NOC)*, pp. 1–6, July 2015.

[11] G. Agrawal, *Fiber-Optic Communication Systems*. New York: Wiley, 4th ed., 2010.

[12] C. Pulikkaseril, L. A. Stewart, M. A. F. Roelens, G. W. Baxter, S. Poole, and S. Frisken, "Spectral Modeling of Channel Band Shapes in Wavelength Selective Switches," *Optics Express*, vol. 19, no. 9, pp. 4–11, April 2011.

[13] T. Zami and B. Lavigne, "Advantages at Network Level of Contentionless $N \times M$ adWSS," *Optical Fiber Communication Conference and Exhibition (OFC)*, San Diego, CA, USA, March 2019, paper M1A.2.

[14] A. Morea, J. Renaudier, T. Zami, A. Ghazisaeidi, and O. Bertran-Pardo, "Throughput Comparison Between 50 GHz and 37.5 GHz Grid Transparent Networks," *J. Opt. Commun. Netw.*, vol. 7, no. 2, pp. A293–A300, February 2015.

[15] T.-W. Yeow, K. Law, and A. Goldenberg, "MEMS Optical Switches," *IEEE Commun. Magazine*, vol. 39, pp. 158–163, November 2001.